SLAC-PUB-1212
(T-E)
March 1973

A Measurement of the $K^o_{\mu 3}/K^o_{e3}$ Branching Ratio, the $K^o_{\ell 3}$ Form Factors, and the $K^o_{\pi 3}$ Decay Parameters*

G.W. Brandenburg, W.B. Johnson, D.W.G.S. Leith, J.S. Loos**
J.A.J. Matthews, F.C. Winkelmann,*** and R.J. Yamartino****

Stanford Linear Accelerator Center
Stanford University, Stanford, California 94305

Abstract

In a hydrogen bubble chamber experiment with a K_L beam we have measured the $K^o_{\mu 3}/K^o_{e3}$ branching ratio to be R = .741 ± .044 and the slope of the f_+ form factor to be λ_+ = .019 ± .013. The data have been analyzed with a new variable, $(p'_T)^2$, which isolates a sample of unique K_{e3} decays and is independent of the K_L beam momentum. These results are compatible with the predictions of K* dominance for f_+ and the Callan-Treiman relation for f_o, but indicate a breaking of the $\Delta I=\frac{1}{2}$ rule. We have also determined the $K_L \rightarrow \pi^+\pi^-\pi^o$/(all charged K_L decays) branching ratio to be R_π = .146 ± .004, and have found the $E^*_{\pi^o}$ slope of the $K_{\pi 3}$ Dalitz plot to be given by g = .73 ± .04.

---

*Work supported by the U.S. Atomic Energy Commission

**Present Address: Duke University, Durham, North Carolina

***Present Address: Lawrence Berkeley Laboratory, Berkeley, California

****Present Address: Purdue University, Lafayette, Indiana

(Submitted to Phys. Rev. D)

I. Introduction

In recent years there have been numerous experimental studies of the semi-leptonic kaon decays, $K \to \pi e \nu$ and $K \to \pi \mu \nu$.[1] One parameter which has remained in doubt, however, is the $K^o_{\mu 3}/K^o_{e3}$ branching ratio (R). This important parameter relates the two $K_{\ell 3}$ form factors, f_+ and f_-, and its comparison with the corresponding ratio for charged K decays is a sensitive test of the $\Delta I = \frac{1}{2}$ rule. In this paper we report a new measurement of R from a high-statistics exposure of a hydrogen bubble chamber to a K_L beam at SLAC. The bubble chamber provides bias-free geometrical acceptance in addition to good momentum resolution.

In order to extract R from the data, we have defined a new variable $(p'_T)^2$ which is independent of the incident K_L momentum and which isolates a sample of unique K_{e3} decays. In addition, the uniquely identified K_{e3} decays are used to determine the slope of the f_+ form factor (λ_+). The slope of the f_o form factor (λ_o) is then derived from our measurements of R and λ_+ and is compared to the Callan-Treiman relation. Finally, using our data for the decay $K_L \to \pi^+ \pi^- \pi^o$, we have measured the branching ratio of charged $K_{\pi 3}$ decays to all charged K_L decays and the $K_{\pi 3}$ Dalitz plot slope parameter.

Section II contains a brief review of $K_{\ell 3}$ phenomenology. The experimental procedures and the kinematical separation of the decay modes are outlined in Section III. The measurement of λ_+ and R are described in Sections IV and V respectively, and these results are discussed in Section VI. The results on the $K_{\pi 3}$ decay mode are presented in Section VII.

II. Phenomenology of $K_{\ell 3}$ Decays

Assuming the pure vector nature of $K_{\ell 3}$ decays, $K \to \pi \ell \nu$, their transition amplitude is given by[1]

$$M \propto \left[(k+q)_\mu \, f_+(t) + (k-q)_\mu \, f_-(t)\right] \bar{u}_\ell \, \gamma_\mu \, (1+\gamma_5) \, u_\nu \qquad (1)$$

where k and q are the four-momenta of the K and π respectively. The form factors, f_+ and f_-, are real functions of t (assuming time reversal invariance); t in turn depends only on the π energy in the K rest frame (E_π^*):

$$t = (k-q)^2 = m_K^2 + m_\pi^2 - 2m_K E_\pi^*. \qquad (2)$$

The transition probability is then

$$\begin{aligned} W &\propto A f_+^2 + B f_+ f_- + C f_-^2 \\ &\propto f_+^2 (A + B\xi + C\xi^2) \end{aligned} \qquad (3)$$

where A, B, and C are functions of the Dalitz plot variables and $\xi = f_-/f_+$. The terms B and C are both proportional to m_ℓ^2; consequently only the f_+ form factor is important for K_{e3} decays. $K_{\mu 3}$ decays, on the other hand, depend on both f_+ and f_-.

The form factors are generally expanded linearly in t:

$$\begin{aligned} f_\pm(t) &\simeq f_\pm(0) \, (1 + \lambda_\pm \, t/m_\pi^2) \\ \xi \, (t) &\simeq \xi(0) + \Lambda \, t/m_\pi^2 \\ \xi \, (0) &= f_-(0)/f_+(0) \\ \Lambda \quad &\simeq \xi(0) \, (\lambda_- - \lambda_+). \end{aligned} \qquad (4)$$

Since $f_+(0)$ is determined by the K_{e3} transition rate, three parameters remain to be determined to first order in t: λ_+, $\xi(0)$, and either λ_- or Λ. Because of the relative insensitivity of the transition

amplitude to f_-, only the first two parameters have been experimentally well determined, and λ_- has been found to be roughly compatible with zero.[1] We assume $\lambda_- = 0$ in the following analysis, although our results would not be affected by values of λ_- similar in magnitude to λ_+. Of the remaining parameters, λ_+ can be obtained from K_{e3} or $K_{\mu 3}$ Dalitz plot studies, while both the $K_{\mu 3}$ Dalitz plot and the μ polarization can be used to determine $\xi(0)$. Assuming μ-e universality, i.e., that f_+ is equal for K_{e3} and $K_{\mu 3}$ decays, then the integration of Eq. (3) over the Dalitz plot yields a quadratic expression for the $K^o_{\mu 3}/K^o_{e3}$ branching ratio in terms of λ_+ and $\xi(0)$:

$$R \simeq .645 + .125\ \xi(0) + .019\ \xi^2(0) + 1.32\ \lambda_+ + .006\ \xi(0)\ \lambda_+. \qquad (5)$$

From a theoretical standpoint a more useful set of form factors is obtained by replacing $f_-(t)$ with

$$\begin{aligned} f_o(t) &= f_+(t) + \frac{t}{m_K^2 - m_\pi^2} f_-(t) \\ &\simeq f_+(0)\ (1 + \lambda_o\ t/m_\pi^2). \end{aligned} \qquad (6)$$

Most predictions are in terms of f_+ and f_o, which are related respectively to the 1^- and 0^+ amplitudes for the lepton pair. In this case the two parameters to be determined are λ_+ and λ_o where

$$\lambda_o = \lambda_+ + \frac{m_\pi^2}{m_K^2 - m_\pi^2}\ \xi(0) \qquad (7)$$

and where the approximation of a linear expansion for f_o corresponds to the assumption that $\lambda_- = 0$. An advantage of this parameterization is that the experimental determinations of λ_+ and λ_o are in general not as highly correlated as those of λ_+ and $\xi(0)$. As an example, the

branching ratio R obtained by substituting (7) into (5) is primarily a function of λ_o:

$$R \simeq .645 + 1.46\,\lambda_o + 2.55\,\lambda_o^2 - .144\,\lambda_+ - 5.03\,\lambda_o\lambda_+ . \qquad (8)$$

In the present experiment we directly measure R and λ_+ and then obtain values for $\xi(0)$ and λ_o using Eqs. (5) and (8) respectively.

A few examples of the many theoretical predictions for the $K_{\ell 3}$ form factors are as follows.[1] $K^*(890)$ dominance of the dispersion relation for f_+ predicts $\lambda_+ \simeq .023$. Current algebra plus PCAC give the Callan-Treiman relation $f_o(m_K^2) \simeq 1.27\, f_o(0)$, where $t = m_K^2$ is outside the physical region. If a linear t dependence is assumed for f_o, then the latter relation implies $\lambda_o = .021$. Finally the $\Delta I = \frac{1}{2}$ rule for leptonic decays predicts that f_+ and f_o for K^o decays be exactly $\sqrt{2}$ times the corresponding form factors for K^+ decays. This in turn predicts that the $K_{\mu 3}/K_{e3}$ branching ratios for K^o and K^+ decays are equal, except for small (< 1%) radiative and phase space corrections. We defer the comparison of these predictions with the experimental data until Sec. VI.

III. Experimental Procedure

A. K_L Bubble Chamber Exposure

The data for this study came from approximately 320K photographs taken in the SLAC 40 in. hydrogen bubble chamber exposed to a K_L beam. These pictures are part of an 800 K picture investigation of $K_L p$ hadronic interactions. The beam was produced by impinging a high-energy electron beam on a Beryllium target 56 m. upstream of the chamber,[2] and yielded approximately 25 K_L per picture. The K_L momentum spectrum, as shown in Fig. 1, peaks at about 4 GeV/c and extends to 12 GeV/c.

The sample of K_L decays has been obtained by scanning for 2-prong (V) events not associated with an interaction in the chamber.[3] No attempt has been made at the scanning stage to identify individual decay modes. These events have been measured on the SLAC spiral reader or on film plane devices and reconstructed using the program TVGP.[4] Any events which failed because of bad measurement have been remeasured. In addition to the present study of the K_L decay parameters, these data have also been used to determine the K_L momentum spectrum by a statistical method.[2]

B. Selection of K_L Decays

For an event to be selected as a K_L beam decay it must be compatible within measurement errors with any of the decay modes $\pi e \nu$, $\pi \mu \nu$, or $\pi^+ \pi^- \pi^o$. However, since the beam momentum is unknown no kinematic fitting is possible. In order to remove γ conversions and K_S and Λ decays, any events satisfying the following mass cuts have been excluded from the data:

$$M(e^+e^-) < 35 \text{ MeV}$$

$$485 < M(\pi^+\pi^-) < 510 \text{ MeV}$$

$$1110 < M(p\pi^-) < 1120 \text{ MeV},$$

where the mass assignments of the charged particles are as indicated. As estimated from the Monte Carlo calculation discussed below, these cuts also remove approximately 8% of the K_L decays. Finally, to avoid events where scanning and/or measuring biases may occur, we have required that both tracks have lab momenta greater than 50 MeV/c and that the lab opening angle be less than 45^o. These cuts eliminate 2% and 5% respectively of the true K_L sample. None of the above cuts strongly affect the Dalitz plot distributions.

Selecting events in this manner we find no evidence of any contamination in the K_L sample above the 1% level as shown in Table I. The only significant bias remaining is an estimated 2 ± 1% loss of K_{e3} decays due to electron Bremsstrahlung near the decay vertex. This is based on the assumption that electron tracks which lose more than ~ 15% of their energy in the first 10 cm will be unmeasureable. Other possible sources of bias, such as non-beam K_L decays, pion decays in flight, and Dalitz pairs from $K_{\pi 3}$ decays are seen to be neglible. The final sample of K_L decays consists of 20193 events.

C. Monte Carlo Simulation

In order to extract the K_L decay parameters from our data, we have generated Monte Carlo events for the three charged K_L decay modes. The $K_{\ell 3}$ matrix elements discussed in Sec. II have been modified by radiative corrections;[5] the $K_{\pi 3}$ matrix element squared is assumed to be linear in the π^o Dalitz plot energy (see Sec. VII) and has been corrected for the Coulomb interaction of the charged pions.[6] The events have been generated using the beam spectrum shown in Fig. 1, after weighting the spectrum by the decay probability. The momentum vectors of both charged particles as well as the K_L beam direction have been perturbed by an amount corresponding to the measurement errors in our experiment. Finally, the Monte Carlo events have been subjected to the same selection criteria as the data sample.

The measurement errors for the charged tracks have been parameterized as a function of momentum by averaging the track errors for actual events. These errors, which are computed by the reconstruction program TVGP,[4] are a combination of the setting error and the uncertainty due to multiple

scattering. To check the error parameterization, we have investigated the width of the $K_S \rightarrow \pi^+\pi^-$ peak shown in Fig. 2, where no K_L decay restriction has been applied to the data. The curve shows the Monte Carlo prediction for K_S decays generated according to the observed K_S momentum spectrum and normalized to the K_S peak. The experimental mass resolution is seen to be adequately reproduced by the Monte Carlo program.

In addition to the track measurement error, there is also a small uncertainty in the direction of the K_L beam. This results from the slight jitter of the film position relative to the chamber and not from the negligible size of the target, which is 56 m upstream. The size of this effect has been determined by plotting the missing transverse momentum for the kinematically overconstrained events of the type $K_L p \rightarrow K^{\pm}\pi^{\mp}p$. This is shown in Fig. 3, where p_y (p_z) is the momentum component transverse to the beam and parallel (perpendicular) to the film plane. It is found that a beam direction uncertainty of 1 mrad (2 mrad) in the y (z) direction correctly predicts the widths of these distributions when added in quadrature to the track errors discussed above, as shown by the curves in Fig. 3. Consequently, the beam direction in the Monte Carlo program has been perturbed by the same amount.

Finally, to demonstrate that the Monte Carlo simulation is in good agreement with the K_L data, Figs. 4 and 5 show the lab momenta and opening angle distributions for $K_{\ell 3}$ decays selected by the requirement $(p_o')^2 < -.008$ GeV^2 (see following section). The curves are the predicted shapes using the decay parameters discussed below. The positive and negative track momenta have been plotted separately in Figs. 4a and 4b respectively, although they are predicted to have the same shape within

the accuracy of our experiment. There are no significant discrepancies between the data and the predictions for these variables or for any of the variables used in the subsequent analysis. Therefore, we can determine the decay parameters by comparing the data with the predictions of the Monte Carlo program, confident that it effectively simulates the experimental conditions.

D. Separation of Decay Modes

It is well known that the variable $(p_o')^2$ is useful for separating the $K_{\pi 3}$ decay mode from both $K_{\ell 3}$ modes.[7] This variable is defined as the K_L momentum squared in the frame where the π^o momentum is transverse to the beam direction, assuming a $K_{\pi 3}$ decay (see Appendix). Neglecting resolution effects, $K_{\pi 3}$ decays are restricted to positive values of $(p_o')^2$, whereas K_{e3} and $K_{\mu 3}$ decays are concentrated at negative $(p_o')^2$ values. The $(p_o')^2$ distribution obtained in this experiment is shown in Fig. 6. The solid curve is the prediction of the Monte Carlo simulation using the parameters determined in the following sections. The $K_{\ell 3}$ background for $(p_o')^2 > 0$ comprises approximately 20% of the sharp $K_{\pi 3}$ peak, as shown by the dashed curve. The selection $(p_o')^2 < -.008$ GeV^2 removes more than 99% of the $K_{\pi 3}$ decays but retains ~ 94% of the $K_{\ell 3}$ decays, leaving a sample of 15800 unique $K_{\ell 3}$ decays.

Although it is possible to determine the $K^o_{\mu 3}/K^o_{e3}$ branching ratio by fitting the negative range of $(p_o')^2$ to the sum of the expected distributions for K_{e3} and $K_{\mu 3}$,[7] this procedure has two drawbacks. First, the $(p_o')^2$ distribution for $K_{\ell 3}$ decays is not independent of the beam spectrum. Thus any uncertainty in the indirect determination of the beam spectrum will be reflected in a fit to $(p_o')^2$. Second, $(p_o')^2$ does not provide a

well-defined separation of the two $K_{\ell 3}$ modes. To circumvent these difficulties we define a new variable, $(p'_T)^2$, which depends only on the transverse momenta:

$$
\begin{aligned}
(p'_T)^2 &\equiv C_T^2 - p_T^2 \\
C_T &\equiv m_K - \sqrt{p_{1T}^2 + m_\pi^2} - \sqrt{p_{2T}^2 + m_\mu^2} \\
p_{1T} &> p_{2T}.
\end{aligned}
\tag{9}
$$

Here p_T is the transverse momentum of the neutral particle (ν or π^o) and C_T is a cutoff depending on p_{1T} and p_{2T}, the transverse momenta of the two charged particles. Since there are no longitudinal momentum components in this definition, $(p'_T)^2$ is clearly independent of the beam momentum and has the useful property that $K_{\mu 3}$ decays are restricted to positive values. To show this we write for a $K_{\mu 3}$ decay in its rest frame

$$
\begin{aligned}
p_\nu^* = E_\nu^* &= m_K - E_\pi^* - E_\mu^* \\
&= m_K - \sqrt{p_\pi^{*2} + m_\pi^2} - \sqrt{p_\mu^{*2} + m_\mu^2}
\end{aligned}
\tag{10}
$$

from which it follows that

$$
p_T \leq p_\nu^* \leq m_K - \sqrt{p_{\pi T}^2 + m_\pi^2} - \sqrt{p_{\mu T}^2 + m_\mu^2} \, . \tag{11}
$$

Since it is not possible to distinguish the π from the μ, the larger permutation of the right-hand side of (11) is given by our definition of C_T in Eq. (9). Therefore, $(p'_T)^2 \geq 0$ for all $K_{\mu 3}$ decays, neglecting experimental resolution. Since p_T can in general be larger in K_{e3} decays than in $K_{\mu 3}$ decays, a region of unique K_{e3} decays exists for negative values of $(p'_T)^2$.

In Fig. 7 we show a scatter plot of $(p'_T)^2$ versus $(p'_o)^2$ to illustrate

the relationship of these variables. The axes of this plot are seen to be kinematical boundaries for the $K_{\mu 3}$ and $K_{\pi 3}$ decay modes, while K_{e3} decays populate all regions of the plot. Selecting events with $(p_T')^2 < -.004$ GeV^2 results in a sample of 1871 K_{e3} decays, with less than 3% $K_{\mu 3}$ contamination. The efficiency of this kinematical cut for selecting K_{e3} decays as a function of E_π^* and t is shown by the solid curve in Fig. 8b, while the pion energy spectrum is shown in Fig. 8a. The efficiency varies gradually across the Dalitz plot and averages about 15% for all K_{e3} decays.

IV. Determination of λ_+

As discussed in Sec. II, K_{e3} decays depend only on the f_+ form factor and not on f_-. To determine the parameter λ_+ in the linear expansion of f_+ we have used the unique K_{e3} events isolated as discussed above. In order to reduce contamination from the spillover of poorly measured $K_{\mu 3}$ events to negative values of $(p_T')^2$, we have accepted only those events with $(p_T')^2 < -.004$ GeV^2. The remaining $K_{\mu 3}$ contamination ($< 3\%$) has been taken into account in the fits to the data.

The events selected in this manner are highly transverse, i.e. the decay plane is in general perpendicular to the beam direction in the K_L rest frame. Because of the large mass difference between the pion and the electron, the Lorentz transformation to the lab then has the interesting property that $\sim 94\%$ of the time the pion track has a higher lab momentum than the electron track. In addition, the transverse nature of the unique K_{e3} decays implies that $p_\pi^* \approx p_{\pi T}$, where p_π^* is the pion momentum in the K_L rest frame. Thus, the p_T distribution of the higher

momentum track in the lab is closely related to the p_π^* distribution and therefore to the t distribution (see Eq. (2)). Identifying the pion in this manner is reliable for values of t smaller than about 5 m_π^2, but is inefficient for larger t. This can be seen from the dashed curve in Fig. 8b, which shows the percentage of all K_{e3} decays which satisfy the unique K_{e3} selection criteria and where $p_\pi > p_e$ in the lab.

The transverse momentum (p_T) distribution of the higher momentum track for the unique K_{e3} sample is shown in Fig. 9. To determine λ_+ we have fit this distribution to the expression

$$Z(p_T) = f_+^2(0) \left[< A > + 2\frac{\lambda_+}{m_\pi^2} < tA > + \frac{\lambda_+^2}{4 m_\pi} < t^2 A > \right] \qquad (12)$$

where the symbol < > indicates the Monte Carlo generated distribution for p_T. A and t are functions of the Dalitz plot variables as defined in Eqs. (2) and (3). A least squares fit has been performed in the interval $20 < p_T < 235$ MeV/c (solid curve in Fig. 9) yielding the result $\lambda_+ = .019 \pm .013$ with a χ^2 of 22 for 29 degrees of freedom (DF).[9]

The error on λ_+ is predominantly statistical with additional contributions from the uncertainties in the $K_{\mu 3}$ contamination (.004) and the Monte Carlo error parameterization (.004). A fit to the more limited sample defined by $(p_T')^2 < -.006$ GeV^2, where the $K_{\mu 3}$ contamination is negligible, gave the same value for λ_+ indicating that the $K_{\mu 3}$ background has been correctly treated. Since only transverse momenta are used in both the event selection and the λ_+ fit, the result is independent of the shape of the beam spectrum except for negligible momentum dependence of resolution effects. It is, however, sensitive to the K_{e3} radiative corrections,[5] which modify the expected shape of the p_T distribution.[10]

V. Determination of the $K^o_{\mu 3}/K^o_{e3}$ Branching Ratio

We have determined the $K^o_{\mu 3}/K^o_{e3}$ branching ratio (R) by fitting the experimental $(p'_T)^2$ distribution to a sum of the expected distributions for K_{e3} and $K_{\mu 3}$ decays. The data are shown in Fig. 10, where the $K_{\pi 3}$ events have been removed by the requirement $(p'_o)^2 < -.008$ GeV^2. The dotted and dashed curves show the respective K_{e3} and $K_{\mu 3}$ contributions, while the solid curve represents their sum. As discussed in Sec. III D, the fact that $K_{\mu 3}$ decays are limited to the positive range of this variable makes it particularly sensitive to R.

In order to calculate the expected $(p'_T)^2$ distributions it is necessary to assume values for λ_+ and $\xi(0)$. We take the value of λ_+ determined from our sample of unique K_{e3} events (see Sec. IV). The result we obtain for R is strongly dependent on the value assumed for λ_+, with a correlation $dR/d\lambda_+ \simeq -1.0$.[11] On the other hand, while the normalization of the $(p'_T)^2$ distribution for $K_{\mu 3}$ decays depends on $\xi(0)$, the shape of the distribution does not. Therefore, our result for R is insensitive to the value of $\xi(0)$ used in the simulation.

A fit of the $(p'_T)^2$ distribution in the range $-.022 < (p'_T)^2 < .054$ GeV^2 is shown by the curve on Fig. 10. This fit yields an uncorrected ratio $R = .758 \pm .038$ with a χ^2 of 101 for 74 DF. The error is the statistical error multiplied by the factor $\sqrt{\chi^2/DF}$ to account for possible systematic errors in the data.[12]

To obtain a final ratio we have adjusted R by $-2 \pm 1\%$ to correct for K_{e3} decays which have unmeasurable electron tracks due to large Bremsstrahlung losses near the decay vertex. The following contributions have then been added in quadrature to the fitted error on R: .013 from

the error in our determination of λ_+, .014 from the uncertainty in the Monte Carlo error parameterization, and .007 from the uncertainty in the Bremsstrahlung correction. The final result is R = .741 ± .044. As with λ_+, the dependence of R on the beam spectrum is negligible. However, the fitted value of R is sensitive to the radiative corrections,[5] which tend to shift K_{e3} events toward negative values of $(p'_T)^2$.[10]

VI. Discussion of $K_{\ell 3}$ Form Factors

In this experiment we have measured both the parameter λ_+ and the $K^o_{\mu 3}/K^o_{e3}$ branching ratio (R). Using the sample of unique K_{e3} decays we have obtained the value $\lambda_+ = .019 \pm .013$ for the slope of the f_+ form factor. This is shown in Fig. 11 together with previous measurements[7,13,14] and the average K^+_{e3} value[1] (dashed line). Our result is in agreement with the prediction of K* dominance (.023) and with the average charged K value. We are also compatible with previous K^o_{e3} measurements with the exception of the recent experiments of Albrow et al. and Dally et al.,[14] which find values approximately two standard deviations larger.

Our value for the branching ratio, R = .741 ± .044, has been determined by fitting the $(p'_T)^2$ distribution. This result is plotted in Fig. 12 along with the results of previous experiments[7,15] and the average ratio from charged K decays[1] (dashed line). Our ratio is larger than the more recent measurements, but agrees with the trend of earlier measurements that the $K_{\mu 3}/K_{e3}$ ratio is larger for neutral decays than for charged decays. This suggests that the $\Delta I=\frac{1}{2}$ rule, which predicts equal neutral and charged ratios, is not exactly satisfied by $K_{\ell 3}$ decays.

Since the neutral and charged K results for λ_+ are compatible, the fact that R depends only on λ_+ and λ_o (see Eq. (8)) implies that any breaking of the $\Delta I=\frac{1}{2}$ rule results from the f_o form factor. This might be the consequence of the absence of a strong $I=\frac{1}{2}$ pole in the f_o dispersion relation, which relates f_o to the S-wave $K\pi$ system. The f_+ dispersion relation, on the other hand, is dominated by the $I=\frac{1}{2}$ $K^*(890)$ in the P-wave.

As discussed in Sec. V, our value for R is dependent on the value assumed for λ_+ with a correlation $dR/d\lambda_+ \simeq -1.0$. Our final ratio assumes $\lambda_+ = .019 \pm .013$, as determined from our data. We note that if λ_+ is assumed to be three standard deviations larger, the value obtained for R is still significantly higher than the previous results for both charged and neutral K decays.

Assuming μ-e universality, our results for λ_+ and R used in conjunction with Eqs. (5) and (8) yield the values $\xi(0) = .5 \pm .4$ and $\lambda_o = .06 \pm .03$.[16]. The correlation of these results with λ_+ is stronger for $\xi(0)$ $(d\xi(0)/d\lambda_+ \simeq -20)$ than it is for λ_o $(d\lambda_o/d\lambda_+ \simeq -.6)$. We note that our value for λ_o is consistent with a linear rise of the f_o form factor to the Callan-Treiman point, which would predict $\lambda_o = .021$. Although most previous $K^o_{\mu 3}$ analyses have yielded negative values for $\xi(0)$ and λ_o,[1] the recent $K_{\mu 3}$ Dalitz plot analysis of Donaldson et al.[17] also finds that f_o is greater than $f_+(0)$ throughout the physical region and that f_o extrapolates to the Callan-Treiman point.

VII. Results on $K_L \rightarrow \pi^+\pi^-\pi^o$

In this section we investigate our data on the $K_{\pi 3}$ decay mode, $K_L \rightarrow \pi^+\pi^-\pi^o$. These decays are concentrated at positive values of the variable $(p'_o)^2$, as was discussed in Sec. III D. The experimental $(p'_o)^2$

distribution is shown in Fig. 6. The dashed curve under the $K_{\pi 3}$ peak is the prediction of the Monte Carlo simulation for $K_{\ell 3}$ decays assuming the decay parameters determined in the previous sections. It is seen that the leptonic decays comprise a large (~ 25%), but well-understood background to the $K_{\pi 3}$ decays.

In order to determine the branching ratio, R_π, of $K_L \to \pi^+\pi^-\pi^o$ to all charged K_L modes, we have fitted the $(p'_o)^2$ distribution to a sum of the predicted distributions for the $K_{\pi 3}$ and $K_{\ell 3}$ modes. The simulated $K_{\pi 3}$ events have been generated assuming linear slope for the π^o Dalitz plot energy distribution as described below, and have been weighted to correct for the Coulomb interaction of the charged pions.[6] Fitting the data in the interval $-.060 < (p'_o)^2 < .024$ GeV^2 gives the result $R_\pi = .146 \pm .004$. The fit, which is shown by the solid curve in Fig. 6, has a χ^2 of 115 for 82 DF.[12] The result has been adjusted slightly (-0.5%) to account for the loss of $K_{\pi 3}$ events with Dalitz pairs and of K_{e3} events due to large Bremsstrahlung near the decay vertex (see Table I).

The error on R_π is the sum in quadrature of the statistical error multiplied by $\sqrt{\chi^2/DF}$ and a contribution of .002 arising from the uncertainty in the parameterization of the measurement errors used in the simulation. The result is insensitive to the choice of the $E^*_{\pi o}$ slope parameter, to the $K_{\pi 3}$ Coulomb corrections, and to the uncertainty in the shape of the beam spectrum. Also, variation of the $K_{\ell 3}$ decay parameters within several times their errors or omission of the $K_{\ell 3}$ radiative corrections does not significantly change the value of R_π.

Our result is significantly smaller than the World Average,[18] $R_\pi = .161 \pm .004$. As we believe that the $K_{\ell 3}$ background under the $K_{\pi 3}$

peak can be accurately predicted, such a discrepancy could only arise in our experiment from a loss of $K_{\pi 3}$ events at the scanning or measuring stage. However, in general we find that $K_{\pi 3}$ decays are easier to identify and measure than their leptonic counterparts. Furthermore, even if we assume that all $K_{\pi 3}$ events with Dalitz pairs were lost (we estimate that at least half are saved by careful scanning), R_{π} would be increased by less than a percent. We do note that our measurement is based on approximately twice as many events as the best previous measurement.

As mentioned above, we have parameterized the deviation of the $K_{\pi 3}$ transition probability from pure phase space as[18]

$$W \propto 1 + g \frac{S_{12} - S_0}{m_\pi^2}$$

$$S_{12} = m_K^2 + m_\pi^2 - 2m_K E^*_{\pi o} \qquad (13)$$

$$S_0 = \frac{1}{3}(m_K^2 + 3m_\pi^2)$$

where S_{12} is the mass squared of the two charged tracks taken as pions. We have determined the parameter g by fitting the $E^*_{\pi o}$ distributions for the $K_{\pi 3}$ sample shown in Fig. 13a, which is defined by $(p'_o)^2 > -.005$ GeV^2. This cut, which leaves 4051 events, retains approximately 98% of the $K_{\pi 3}$ events in the K_L sample but minimizes the $K_{\ell 3}$ background at about 22%. The $E^*_{\pi o}$ distribution is fitted to a sum of $K_{\pi 3}$ events generated according to both phase space and phase space multiplied by $E^*_{\pi o}$, where the relative amounts are given by Eq. (13). To this is added a $K_{\ell 3}$ background component which is fixed by our measurements of λ_+ and R, and which is normalized to the data with $(p'_o)^2 < -.008$ GeV^2. The best fit in the interval $133 < E^*_{\pi o} < 186$ MeV, as shown by the solid curve in Fig. 13a, resulted in the value $g = .73 \pm .04$ with a χ^2 of 66 for 51 DF. The error

is the statistical error from the fit multiplied by $\sqrt{\chi^2/DF}$.

To illustrate the linear nature of the $K_{\pi 3}$ matrix element squared, in Fig. 13b the $E^*_{\pi^o}$ distribution is plotted after subtraction of the expected $K_{\ell 3}$ background and division by $K_{\pi 3}$ phase space. A simple linear fit to this distribution yielded the same result as the fit described above, and is shown by the straight line. In both fits any quadratic dependence on $E^*_{\pi^o}$ was found to be negligible.[19]

If the 4 lowest $E^*_{\pi^o}$ points are eliminated from either fit the results are unchanged, but the χ^2 is decreased to 50 for 47 DF. The fitted value for g is also insensitive to the $K_{\pi 3}$ Coulomb corrections,[6] to the position of the $(p'_o)^2$ cut, and to the uncertainties in the Monte Carlo error parameterization. Furthermore, changing the values of R and R_π by several standard deviations, i.e. altering the amounts of K_{e3} and $K_{\mu 3}$ background, has no effect on g.

Our value, g = .73 ± .04, differs significantly from the World Average,[18] g = .60 ± .03. However, the recent high-statistics experiment of Messner et al.[20] has obtained the value g = .659 ± .004, which is also significantly larger than the World Average. These results emphasize the failure of the $\Delta I=\frac{1}{2}$ rule for $K_{\pi 3}$ decays. This rule relates the values of g for the various charge modes of the $K_{\pi 3}$ decay, and predicts that g = .47 ± .01 on the basis of charged $K_{\pi 3}$ results.[18]

VIII. Conclusions

In a high statistics K_L experiment using a hydrogen bubble chamber we have measured the $K^o_{\mu 3}/K^o_{e3}$ branching ratio (R) and the slope of the f_+ form factor (λ_+). The value we obtain for λ_+, .019 ± .013, is consistent with the predictions of K* dominance and the $\Delta I=\frac{1}{2}$ rule. However, our

branching ratio, $R = .741 \pm .044$, indicates a violation of the $\Delta I=\frac{1}{2}$ rule. Using our results for λ_+ and R we calculate $\lambda_o = .06 \pm .03$, where λ_o is the slope of the f_o form factor. This number is consistent with a linear rise to the Callan-Treiman point. In addition, we have measured the branching ratio of $K_L \to \pi^+\pi^-\pi^o$ to all charged K_L decay modes to be $R_\pi = .146 \pm .004$, and the $E^*_{\pi^o}$ slope of the $K^o_{\pi 3}$ matrix element squared to be $g = .73 \pm .04$. These latter results both differ significantly from previous measurements.

Acknowledgements

We wish to thank D. Hitlin, S. Wojcicki, and R. Zdanis for useful discussions regarding this work, and G. Luste, K. Moriyasu, and W. Smart for their participation in the earlier stages of the experiment. We are grateful for the assistance provided by R. Watt and the crew of the SLAC 40-inch bubble chamber, by J. Brown and the scanning and measuring staff at SLAC, and by D. Johnson for data handling.

Appendix

In this appendix we discuss a slight modification to the definition of $(p_o')^2$ which improves the separation of the $K_{\pi 3}$ and $K_{\ell 3}$ decay modes. This variable is normally defined as[7]

$$(p_o')^2 = \frac{(m_K^2 - m_{\pi o}^2 - m)^2 - 4m_{\pi o}^2 m^2 - 4m_K^2 p_T^2}{4(p_T^2 + m^2)} \tag{A1}$$

where m is the effective mass of the two charged particles assuming they are pions, and p_T is the missing transverse momentum. This can be re-written in the form

$$(p_o')^2 = \frac{m_K^2}{p_T^2 + m^2}(p_{\pi o}^{*2} - p_T^2) \tag{A2}$$

where $p_{\pi o}^*$ is the momentum of the π^o in the K_L rest frame, assuming a $K_{\pi 3}$ decay. In this form it is apparent that true $K_{\pi 3}$ decays are limited to positive values of $(p_o')^2$, since p_T cannot exceed $p_{\pi o}^*$. If we write

$$\begin{aligned} p_{\pi o}^{*2} &= E_{\pi o}^{*2} - m_{\pi o}^2 \\ &= \left(\frac{m_K^2 + m_{\pi o}^2 - m^2}{2m_K}\right)^2 - m_{\pi o}^2 \end{aligned} \tag{A3}$$

we see that when m exceeds its maximum value for a $K_{\pi 3}$ decay, $E_{\pi o}^*$ is less than $m_{\pi o}$ and $p_{\pi o}^{*2}$ becomes negative. However, if m exceeds $m_K + m_{\pi o}$, then $p_{\pi o}^{*2}$ becomes positive again, even though $E_{\pi o}^*$ is negative. Physically this situation corresponds to a K_L π^o collision producing a $\pi^+\pi^-$ pair. Actually, for our range of K_L beam momenta, K_{e3} decays can have large enough "dipion masses" to give positive values of $p_{\pi o}^{*2}$ and $(p_o')^2$. To avoid this possibility we have redefined $(p_o')^2$ as

$$(p_o')^2 = \frac{m_K^2}{p_T^2 + m^2}\left(E^*_{\pi o}\ |E^*_{\pi o}| - m^2_{\pi o} - p_T^2\right) \qquad (A4)$$

which insures that K_{e3} decays with increasingly large values of m will fall at increasingly negative values of $(p_o')^2$. Both the data and the Monte Carlo events have been plotted according to this prescription. The effect of this redefinition is to reduce the fraction of K_{e3} events with $(p_o')^2 > -.008$ GeV^2 from ~ 13% to ~ 4% thereby decreasing the background under the $K_{\pi 3}$ peak. The $(p_o')^2$ distribution for $K_{\mu 3}$ and $K_{\pi 3}$, however, are left unchanged by the new definition. We note that the same effect can be achieved by using only those events with $m < m_K$ when plotting $(p_o')^2$.

In a similar fashion, the variable $(p_T')^2$ defined in Sec. III D, has been computed as $C_T|C_T| - p_T^2$. It is possible for K_{e3} decays with large pion and electron transverse momenta to give negative values of C_T, and the above definition insures that they will be identified as unique K_{e3} decays with $(p_T')^2 < 0$. However, the number of such events is very small (~ 20) and our results are not affected by this modification.

References

1. M.K. Gaillard and L.-M. Chounet, CERN 70-14 (1970);
   L.-M. Chounet, J.-M. Gaillard, and M.K. Gaillard, Phys. Reports 4C, 199 (1972).
2. G.W. Brandenburg, A.D. Brody, W.B. Johnson, D.W.G.S. Leith, J.S. Loos, G.J. Luste, J.A.J. Matthews, K. Moriyasu, B.C. Shen, W.M. Smart, F.C. Winkelmann, and R.J. Yamartino, Phys. Rev. D7, 708 (1973).
3. From a rescan of a fraction of the film the scanning efficiency for unassociated 2-prong events was determined to be 93 ± 1%. The only events excluded from the unassociated 2-prong category were obvious electron pairs (~ 0° opening angle in all views and a low momentum track). We estimate that < .1% of the K_L decays were lost by this criterion.
4. F.T. Solmitz, A.D. Johnson, and T.B. Day, "Three View Geometry Program," LRL Group A Programming Note P-117 (1966), unpublished.
5. E.S. Ginsberg, Phys. Rev. 171, 1675 (1968);
   E.S. Ginsberg, Phys. Rev. 174, 2169 (1968);
   E.S. Ginsberg, Phys. Rev. D1, 229 (1970).
6. A. Neveu and J. Scherk, Phys. Lett. 27B, 384 (1968).
7. D. Luers, I.S. Mittra, W.J. Willis, and S.S. Yamamoto, Phys. Rev. 133B, 1276 (1964);
   H.W.K. Hopkins, T.C. Bacon, and F.R. Eisler, Phys. Rev. Lett. 19, 185 (1967);
   P. Basile, J.W. Cronin, B. Thevent, R. Turlay, S. Zylberajch, and A. Zylbersztejn, Phys. Rev. D2, 78 (1970).

8. Our data cannot distinguish between a linear and a quadratic t dependence for f_+. If a quadratic term $\lambda'_+ t^2/m_\pi^4$, is added to the linear expansion of f_+, the fit allows all reasonable values of λ_+ and λ'_+ which satisfy the empirical relation $\lambda_+ + 4\lambda'_+ \simeq .02$. Equivalently, we have measured the slope of f_+ at an average t of about $2\ m_\pi^2$.

9. The data points for $20 < p_T < 100$ MeV/c have been grouped into four bins for the fit: 20-60, 60-80, 80-90, 90-100 MeV/c.

10. Fits to the data have also been made assuming no radiative corrections to the $K_{\ell 3}$ matrix elements. These yielded the value $\lambda_+ = .027 \pm .014$ and the corrected ratio $R = .705 \pm .044$, however in both cases the χ^2 of the fit was unchanged.

11. If a quadratic expansion of f_+ is assumed, our result for R is independent of small changes in λ_+ and λ'_+ which leave the combination $\lambda_+ + 4\lambda'_+$ constant (see Ref. 8).

12. By determining R and R_π for more restricted ranges of the variables $(p'_T)^2$ and $(p'_o)^2$ respectively (e.g. between -.02 and +.02 GeV^2), the χ^2/DF of the fits can be reduced without affecting the results or their accuracy. On the other hand, the extent to which systematic effects are understood is demonstrated by fitting the entire ranges of these variables, and the fitted errors are then scaled by the factor $\sqrt{\chi^2/DF}$ to account for such uncertainties.

13. G.P. Fisher et al., ANL 7130, p. 83 (1965);
A. Firestone et al., Phys. Rev. Lett. 18, 176 (1967);
J.A. Kadyk et al., Phys. Rev. Lett. 19, 597 (1967);
J.P. Lowys et al., Phys. Lett. 24B, 75 (1967);

H. Aronson et al., Phys. Rev. Lett. 20, 287 (1968);

P. Basile et al., Phys. Lett. 26B, 542 (1968);

V. Bisi et al., Phys. Lett. 36B, 533 (1971);

G. Neuhofer et al., Phys. Lett. 41B, 642 (1972).

14. M.G. Albrow, D. Aston, D.P. Barber, L. Bird, R.J. Ellison, C.H. Halliwell, R.E.H. Jones, A.D. Kanaris, F.K. Loebinger, P.G. Murphy, M.G. Strong, J. Walters, and D.D. Yovanovich, Manchester University Preprint, Paper No. 392 submitted to the XVI Int. Conf. on High Energy Physics, Chicago (1972);

E. Dally,-P. Innocenti, E. Seppi, C.-Y. Chien, B. Cox, L. Ettlinger, L. Resvanis, R.A. Zdanis, C.D. Buchanan, D.J. Drickey, F.D. Rudnick, P.F. Shepard, D.H. Stork, H.K. Ticho, Phys. Lett. 41B, 647 (1972).

15. R.K. Adair et al., Phys. Lett. 12, 67 (1964);

P. Astbury et al., Phys. Lett. 16, 80 (1965);

X. deBouard et al., Nuovo Cimento 52A, 662 (1967);

C.J.B. Hawkins, Phys. Rev. 156, 1444 (1967);

I.A. Budagov et al., Nuovo Cimento 57, 182 (1968);

L.A. Kulyukina et al., JETP 26, 20 (1968);

P. Beilliere et al., Phys. Lett. 30B, 202 (1969);

G.R. Evans et al., Phys. Rev. D7, 36 (1973).

16. We have chosen that solution of the quadratic expression for $\xi(0)$ in Eq. (5) and for λ_o in Eq. (8) which is smaller in magnitude. Furthermore, we have neglected the radiative corrections to these equations (see Ref. 5), which change the results by less than a percent.

17. G. Donaldson, D. Fryberger, D. Hitlin, J. Liu, B. Meyer, R. Piccioni, A. Rothenberg, D. Uggla, S. Wojcicki, and D. Dorfan, SLAC Preprint, Paper No. 779 submitted to the XVI Int. Conf. on High Energy Physics, Chicago (1972).

18. Particle Data Group, Phys. Lett. 39B, 1 (1972).

19. If a term $h(S_{12} - S_0)^2/m_\pi^4$ is added to Eq. (13), the $E^*_{\pi^0}$ fits yield $h = .01 \pm .06$ with no change in g or in the χ^2.

20. R. Messner, A. Franklin, R. Morse, U. Nauenberg, D. Dorfan, D. Hitlin, J. Liu, and R. Piccioni, U. of Colorado Preprint, Paper No. 822 submitted to the XVI Int. Conf. on High Energy Physics, Chicago (1972). These authors find that a quadratic term is necessary to fit the $E^*_{\pi^0}$ distribution.

Figure Captions

1. Momentum spectrum of the K_L beam at the bubble chamber. The error bars represent the uncertainty in the spectrum determination (see Ref. 2).

2. Invariant mass of both charged tracks assuming they are pions. Neither the K_L decay requirement nor the K_S mass cut have been imposed on the data. The curve is the prediction of the Monte Carlo simulation for K_S decays.

3. The components of the missing transverse momentum for events of the type $K_L p \to K^{\pm}\pi^{\mp}p$: (a) $\parallel$ to film plane, (b) $\perp$ to film plane. The curves show the expected widths of these distributions from the track measurement errors plus a small uncertainty in the beam direction.

4. The lab momentum of (a) positive and (b) negative tracks for $K_{\ell 3}$ decays selected by $(p'_o)^2 < -.008$ GeV^2. The curves are the predictions of the Monte Carlo simulation.

5. The opening angle in the lab for $K_{\ell 3}$ decays selected by $(p'_o)^2 < -.008$ GeV^2. The curve is the prediction of the Monte Carlo simulation.

6. $(p'_o)^2$ distribution for entire K_L sample. The solid curve is the Monte Carlo prediction for the sum of all three decay modes, while the dashed curve is the sum of the $K_{\ell 3}$ modes alone for $(p'_o)^2 > -.008$ GeV^2.

7. Scatter plot of $(p'_T)^2$ versus $(p'_o)^2$, where $\sim 1/6$ of the total K_L data are plotted. The decay modes which populate the various sectors are indicated.

8. (a) Dalitz plot energy spectrum of the pion in K_{e3} decays (for $\lambda_+ = .02$). (b) Solid curve shows the efficiency of the unique K_{e3}

selection, i.e. the percentage of K_{e3} decays satisfying $(p'_T)^2 < -.004$ GeV^2 and the cuts discussed in Sec. III B. Dashed curve shows the fraction of K_{e3} decays which satisfy the unique K_{e3} criteria and where the pion has a larger lab momentum than the electron.

9. Transverse momentum of the track with the larger lab momentum for the unique K_{e3} sample selected by $(p'_T)^2 < -.004$ GeV^2. The solid curve is the result of the λ_+ fit described in the text.

10. $(p'_T)^2$ distribution for the $K_{\ell 3}$ sample defined by $(p'_o)^2 < -.008$ GeV^2. The solid curve is the fitted sum of the $K_{\ell 3}$ decay modes, and the dotted and dashed curves show the respective K_{e3} and $K_{\mu 3}$ components.

11. Comparison of the present measurement of λ_+ with the results of previous K^o_{e3} experiments (Refs. 7,13,14). The dashed line is the average λ_+ obtained from charged K_{e3} decays (Ref. 1).

12. Comparison of the $K^o_{\mu 3}/K^o_{e3}$ branching ratio (R) obtained in this experiment with previous measurements (Refs. 7,15). The dashed line is the average $K_{\mu 3}/K_{e3}$ ratio from charged decays (Ref. 1).

13. (a) $E^*_{\pi^o}$ distribution for the $K_{\pi 3}$ sample defined by $(p'_o)^2 > -.005$ GeV^2. (b) Same data after subtraction of the expected $K_{\ell 3}$ background and division by Coulomb corrected $K_{\pi 3}$ phase space. The solid curves are the results of the $K_{\pi 3}$ matrix element fits described in the text.

Table I

Estimated Contaminations and Losses

Final K_L Sample

Contamination	Fraction
Non-beam K_L decays	.003 ± .002
Dalitz pairs from $K_L \rightarrow 3\pi^o$	.002 ± .001
γ, K_S, Λ tails outside mass cuts	< .001
Radiative K_S decays	< .001
$K_L p \rightarrow K^{\pm}\pi^{\mp} p$ with invisible recoil proton	< .001
Loss	**Fraction**
K_{e3} with large Bremsstrahlung near K_L decay vertex	.02 ± .01 (of K_{e3})
Pion decays near K_L decay vertex	.004 ± .002
$K_L \rightarrow \pi^+\pi^-\pi^o$ with Dalitz pairs	.005 ± .002 (of $K_{\pi 3}$)
K_L decay scanned as "obvious electron pair"	< .001

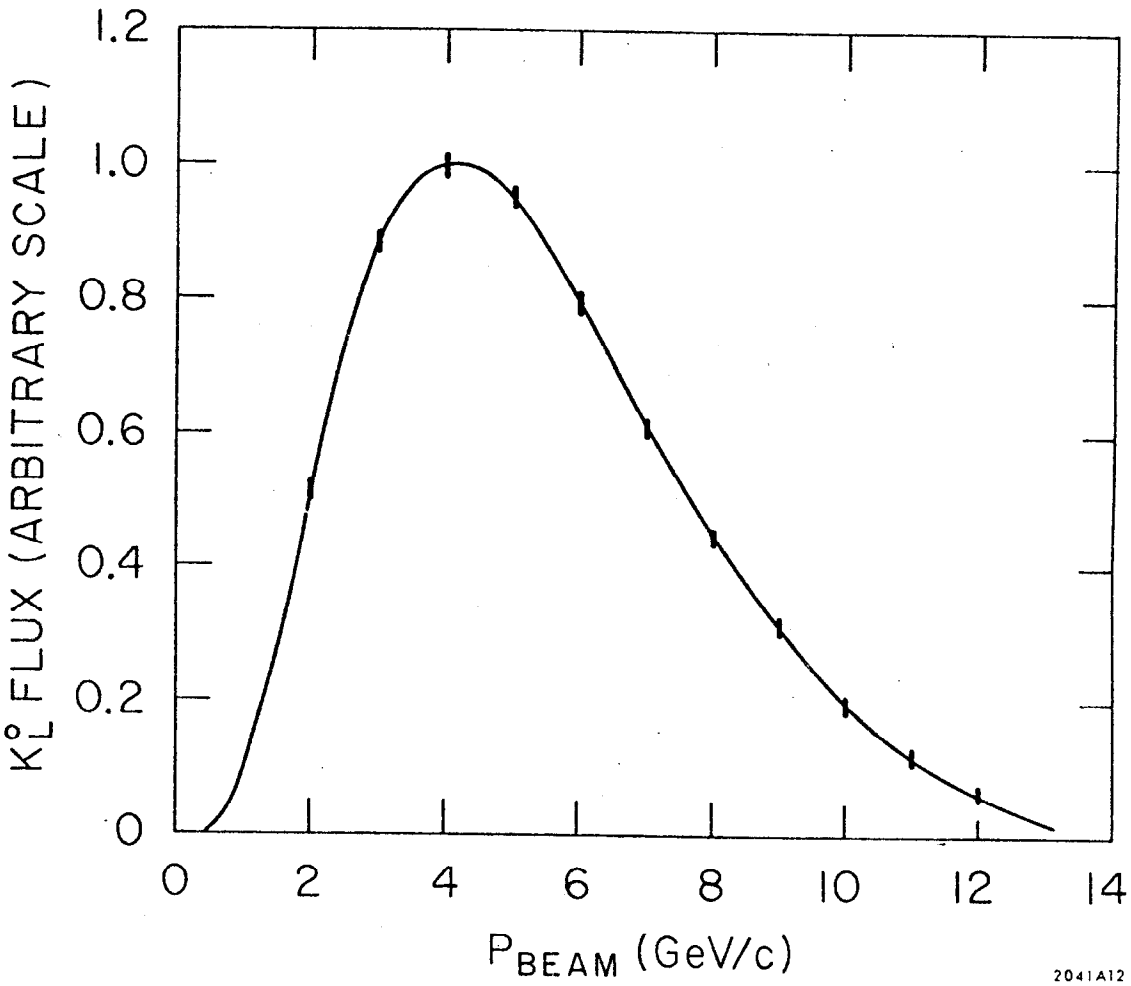
1.2
1.0
0.8
0.6
0.4
0.2
0
K^0_L FLUX (ARBITRARY SCALE)
0
2
4
6
8
10
12
14
P_{BEAM} (GeV/c)
2041A12

Fig. 1

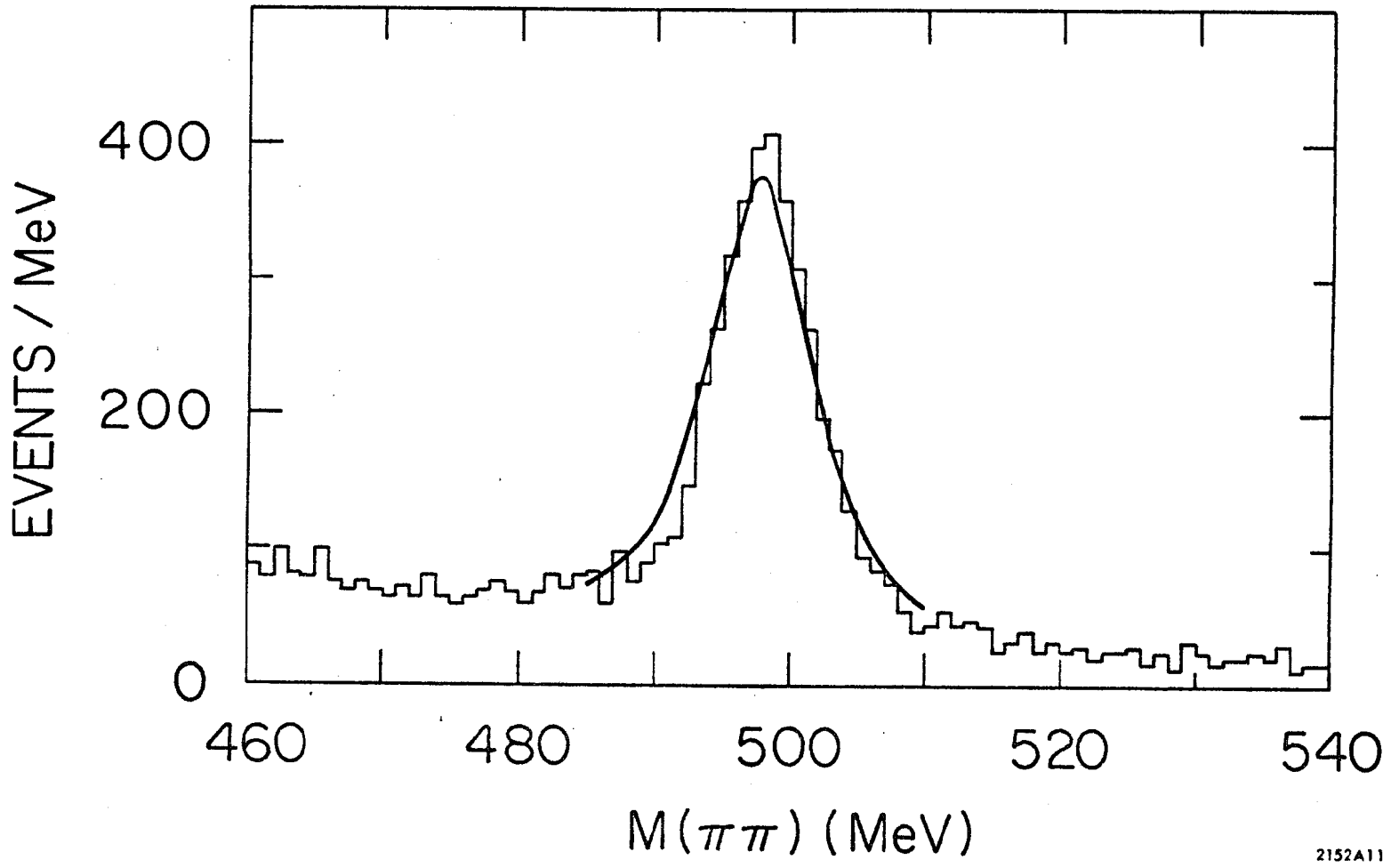

Fig. 2

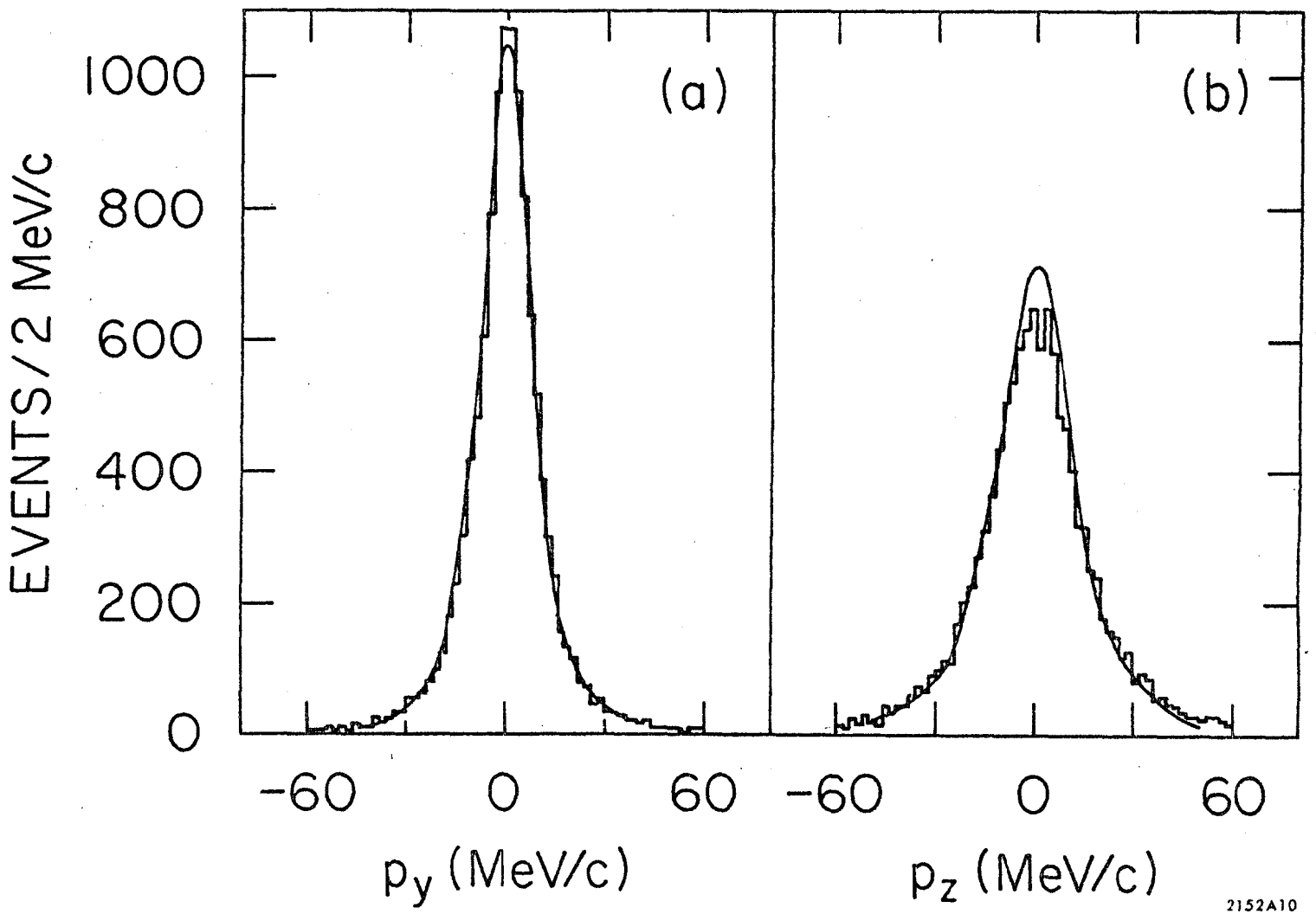
EVENTS/2 MeV/c
1000
800
600
400
200
0
(a)
(b)
-60
0
60
-60
0
60
p_y (MeV/c)
p_z (MeV/c)
2152A10

Fig. 3

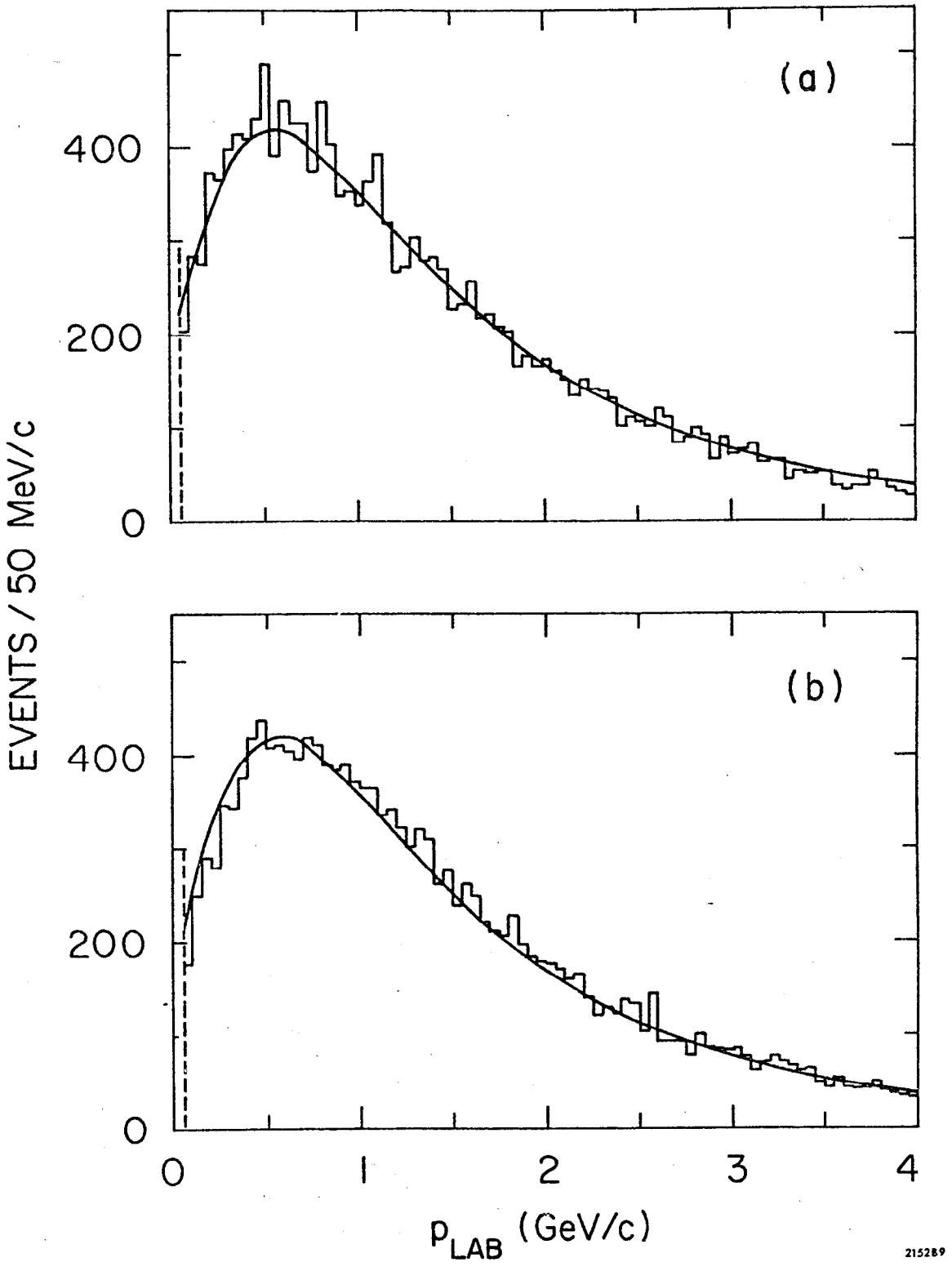

Fig. 4

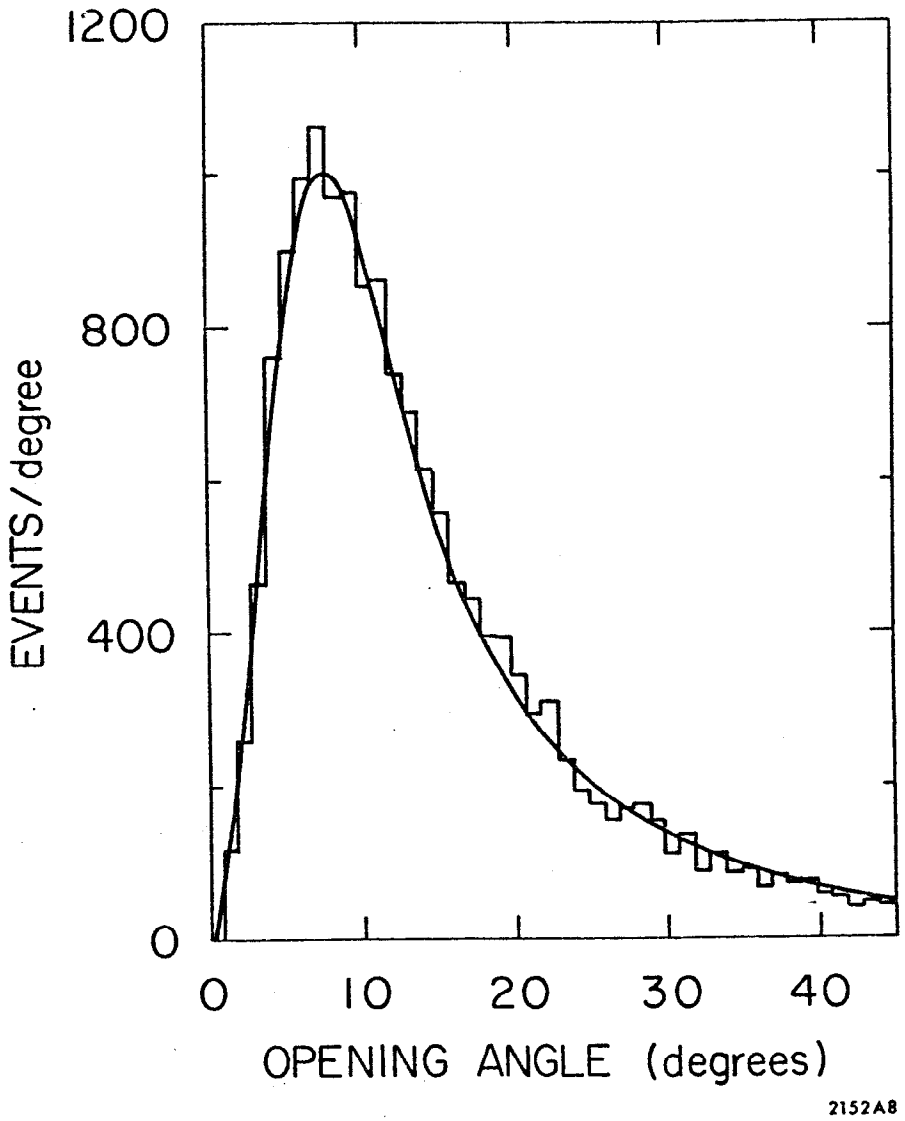
1200
800
400
0
EVENTS / degree
0
10
20
30
40
OPENING ANGLE (degrees)
2152A8

Fig. 5

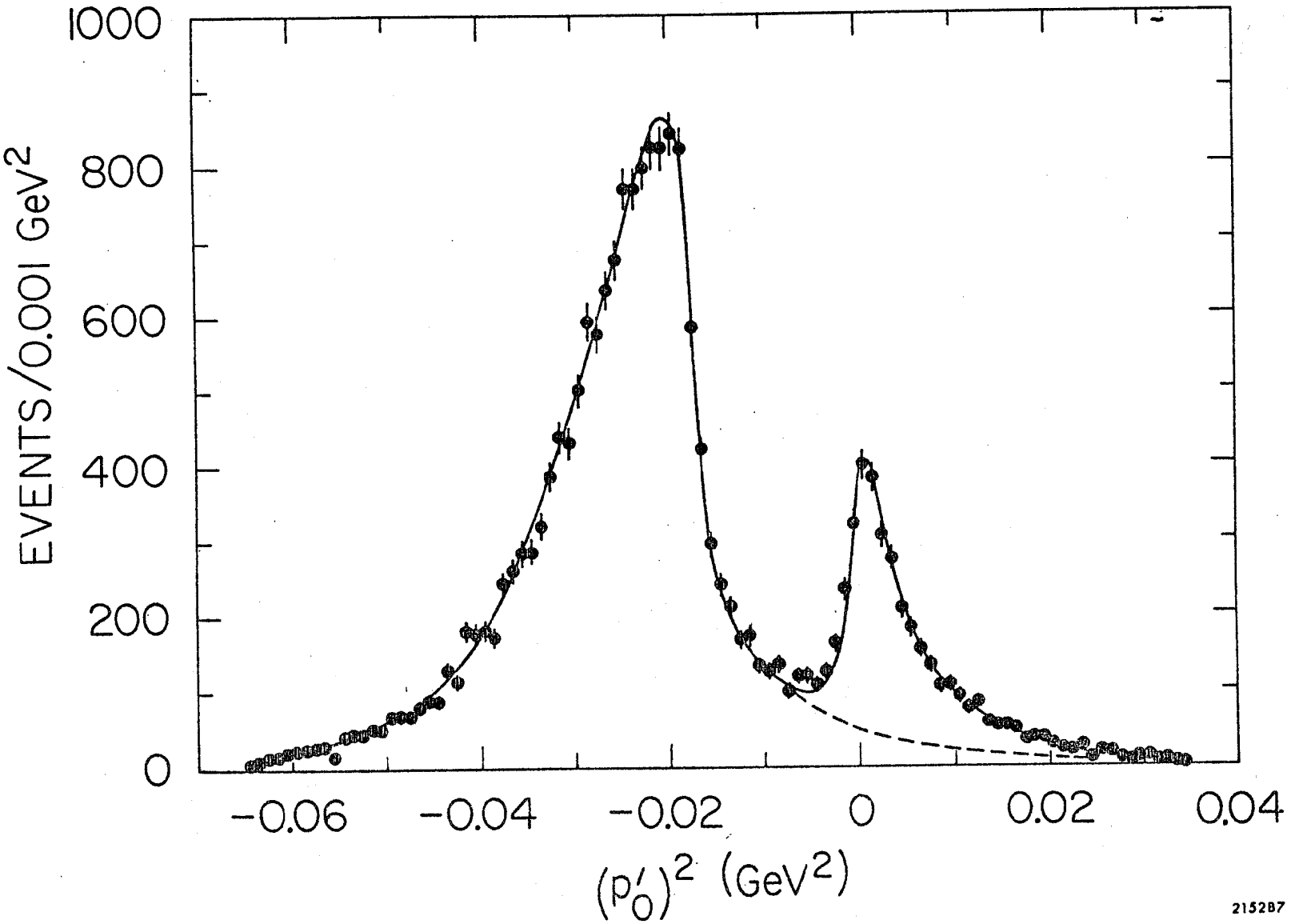
1000
800
600
400
200
0
EVENTS/0.001 GeV²
-0.06
-0.04
-0.02
0
0.02
0.04
(p'0)² (GeV²)
215287

Fig. 6

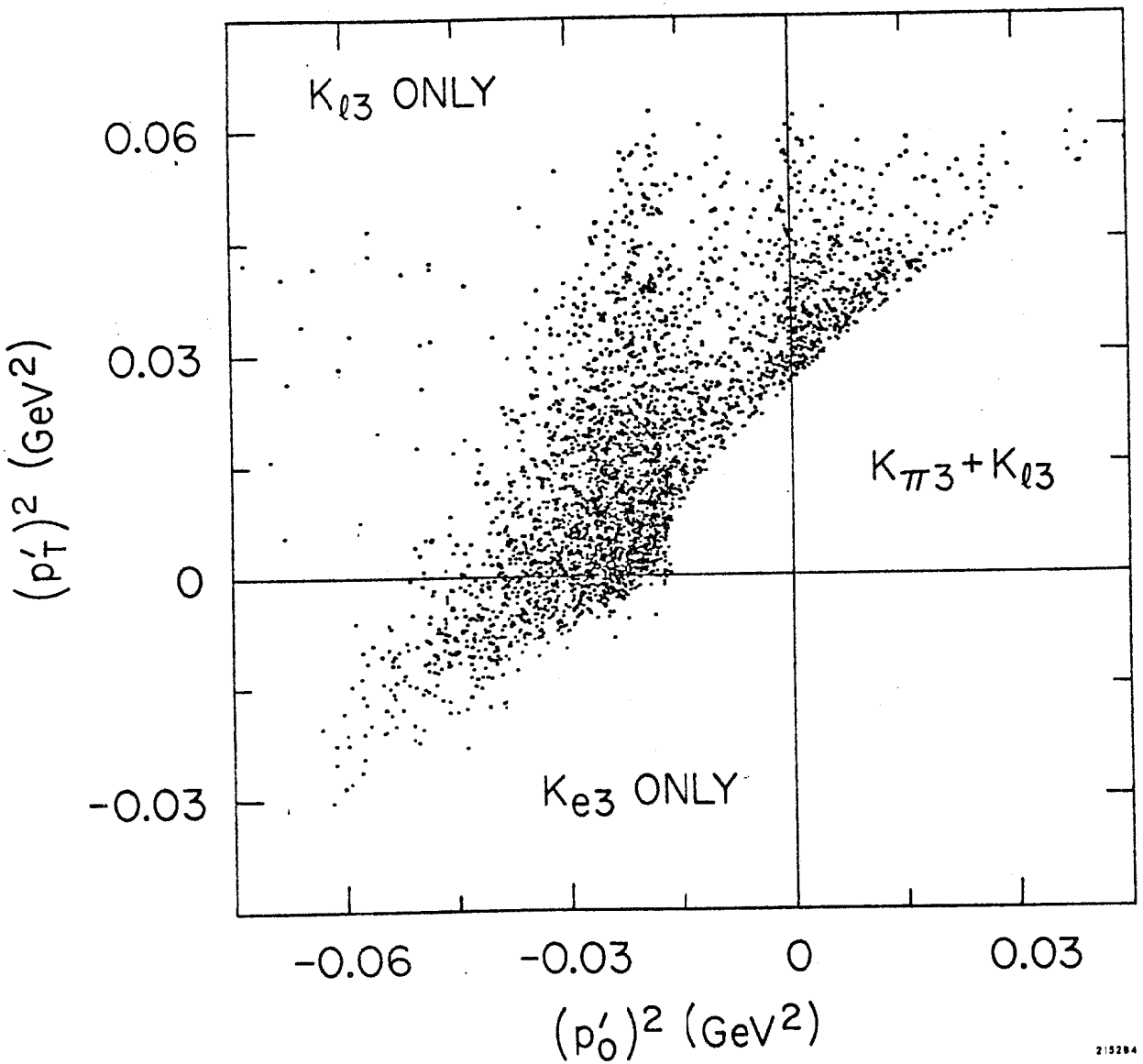
$K_{\ell 3}$ ONLY
$K_{\pi 3}+K_{\ell 3}$
K_{e3} ONLY
0.06
0.03
0
-0.03
$(p'_T)^2$ (GeV^2)
-0.06
-0.03
0
0.03
$(p'_0)^2$ (GeV^2)
215284

Fig. 7

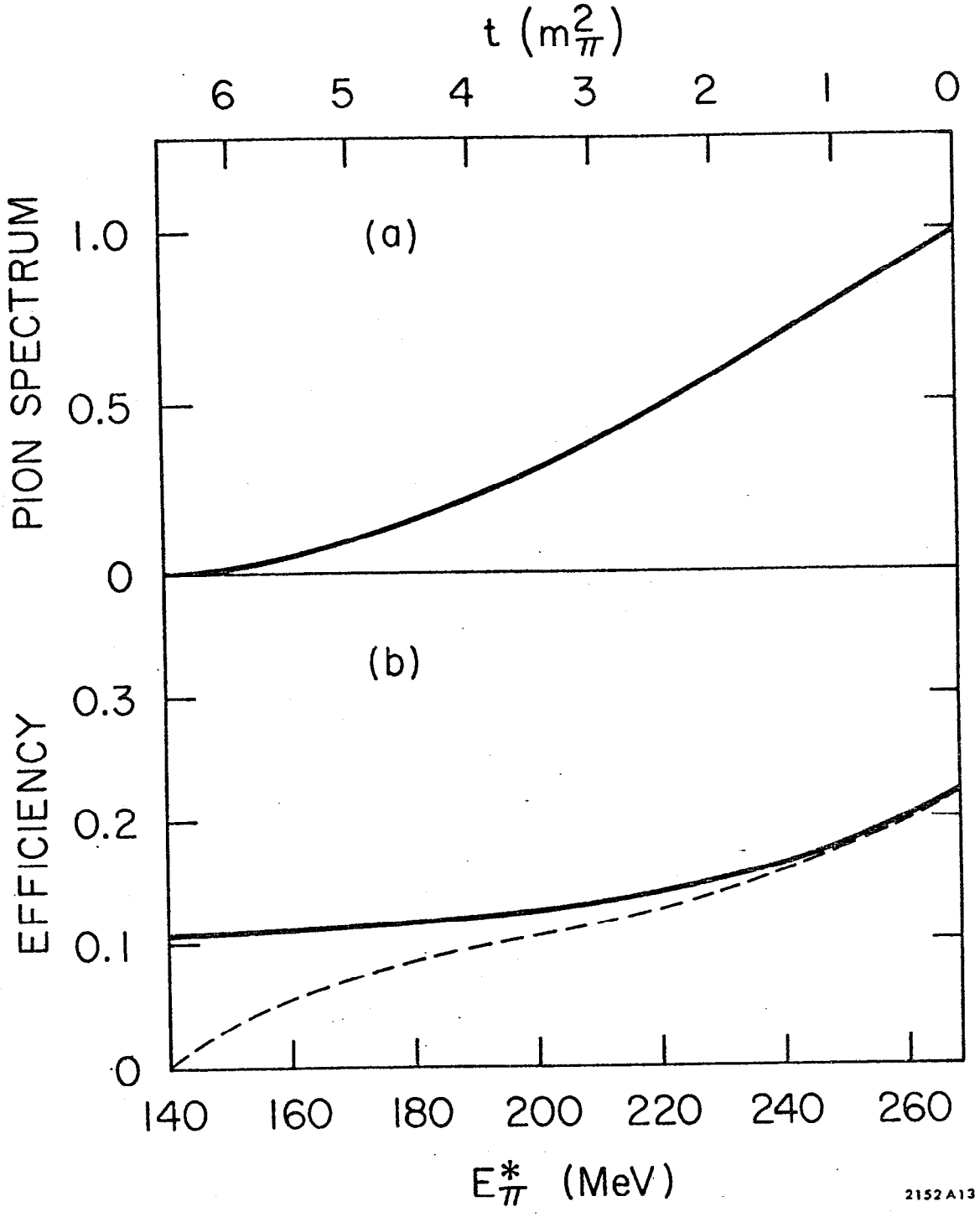
t (m_π^2)
6
5
4
3
2
1
0
PION SPECTRUM
1.0
0.5
0
(a)
(b)
EFFICIENCY
0.3
0.2
0.1
0
140
160
180
200
220
240
260
E_π^* (MeV)
2152A13

Fig. 8

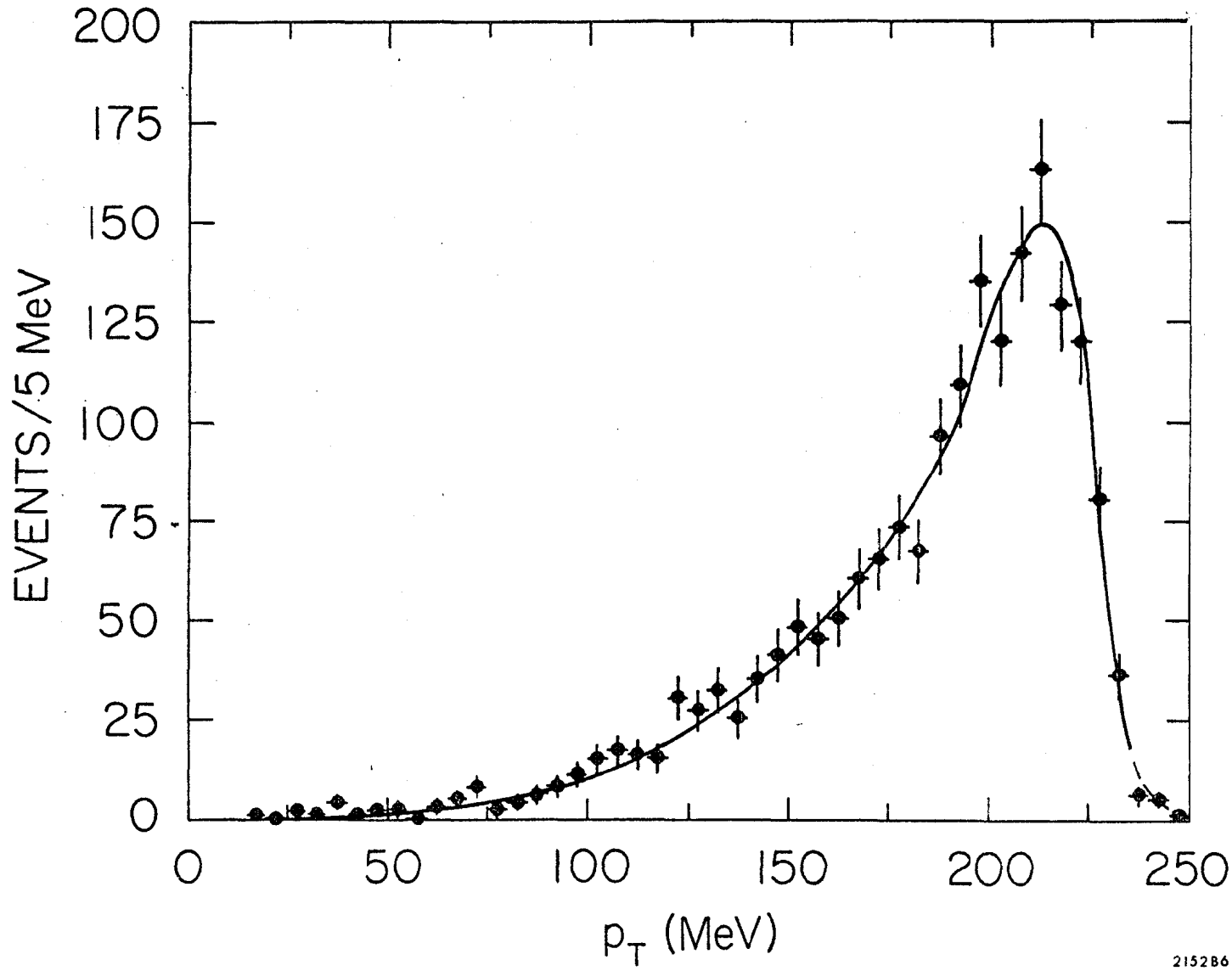
200
175
150
125
100
75
50
25
0
EVENTS/5 MeV
0
50
100
150
200
250
p_T (MeV)
215286

Fig. 9

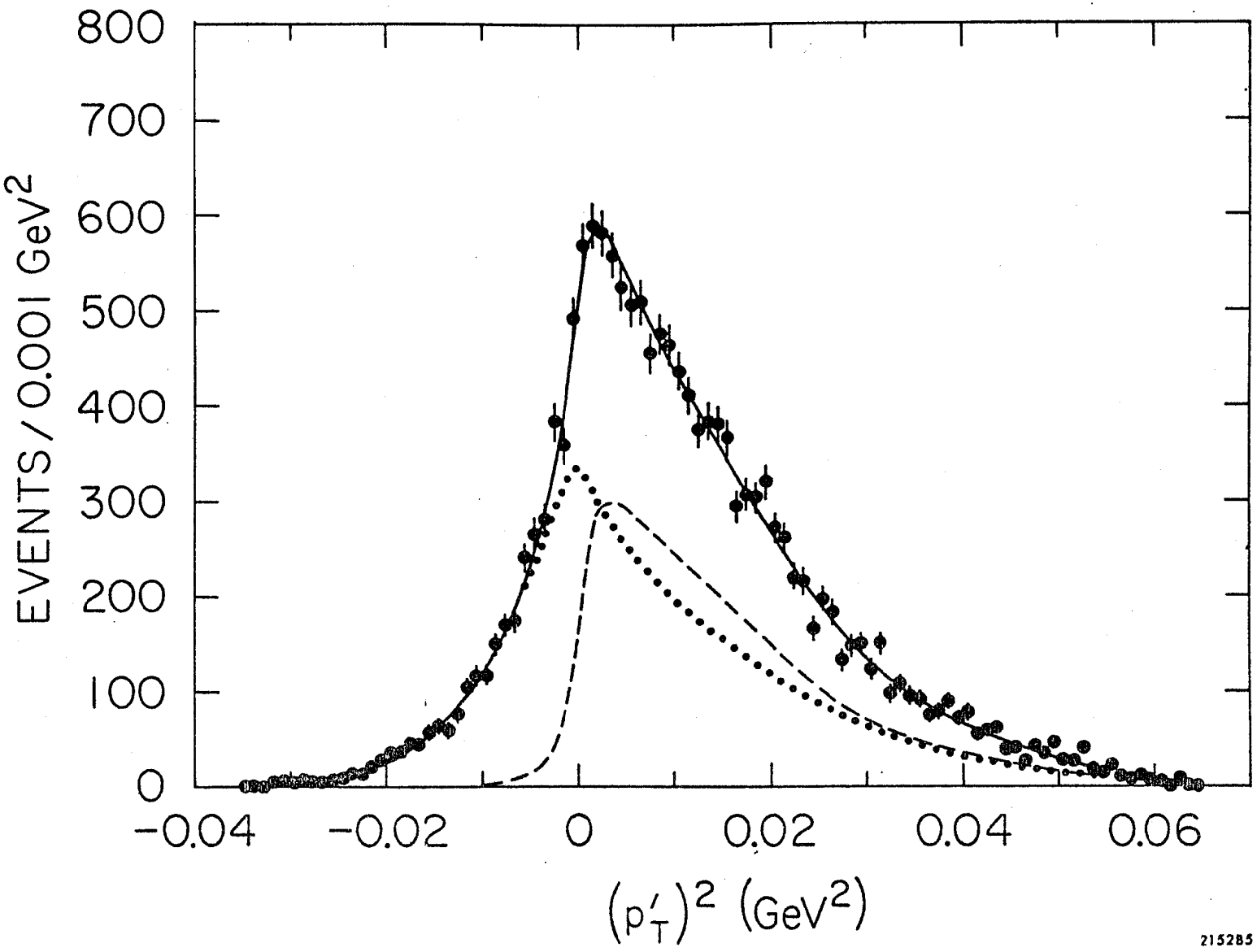
800
700
600
500
400
300
200
100
0
EVENTS / 0.001 GeV^2
-0.04
-0.02
0
0.02
0.04
0.06
$(p'_T)^2$ (GeV^2)
215285

Fig. 10

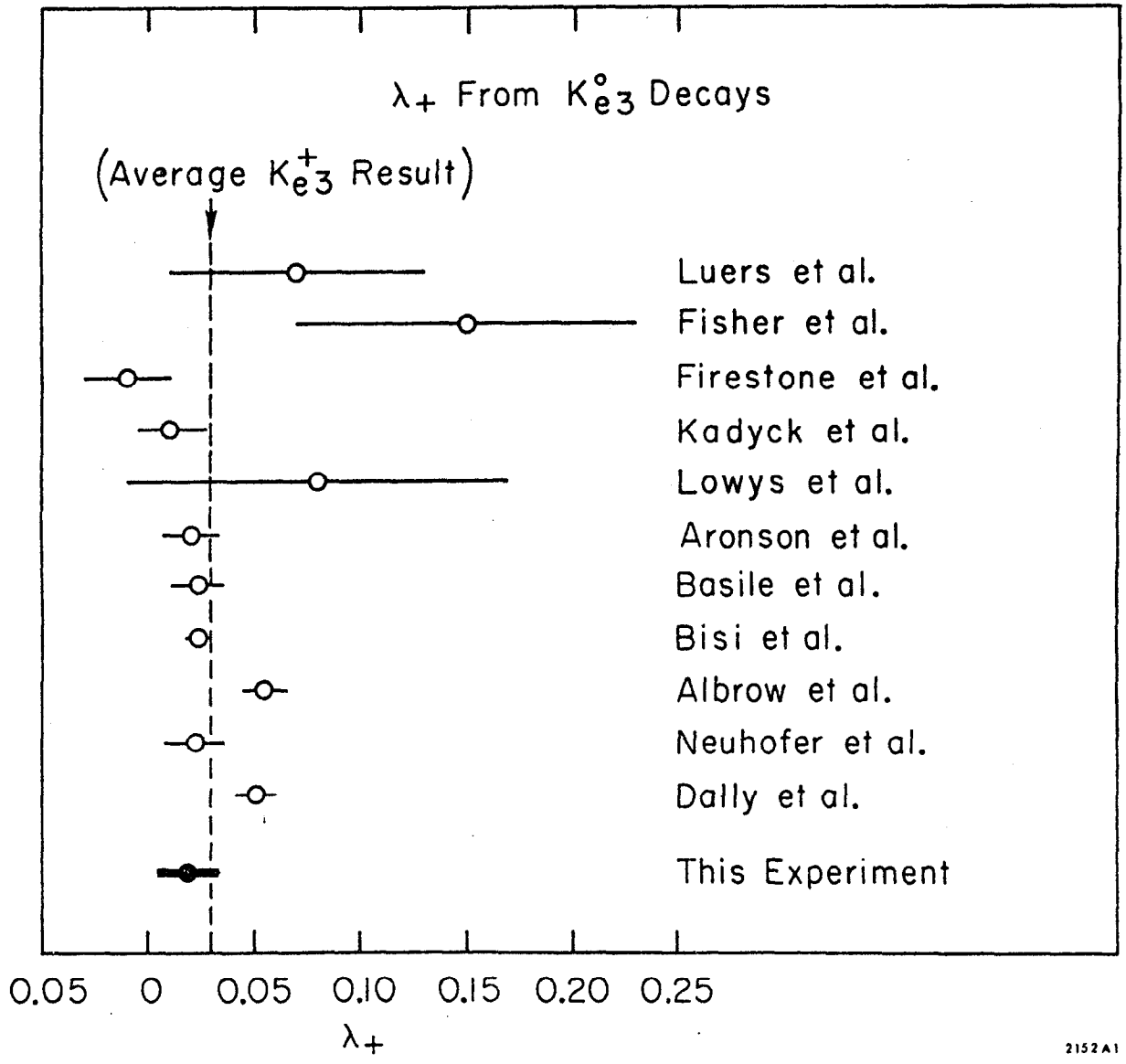
λ+ From K°e3 Decays
(Average K+e3 Result)
Luers et al.
Fisher et al.
Firestone et al.
Kadyck et al.
Lowys et al.
Aronson et al.
Basile et al.
Bisi et al.
Albrow et al.
Neuhofer et al.
Dally et al.
This Experiment
0.05
0
0.05
0.10
0.15
0.20
0.25
λ+
2152A1

Fig. 11

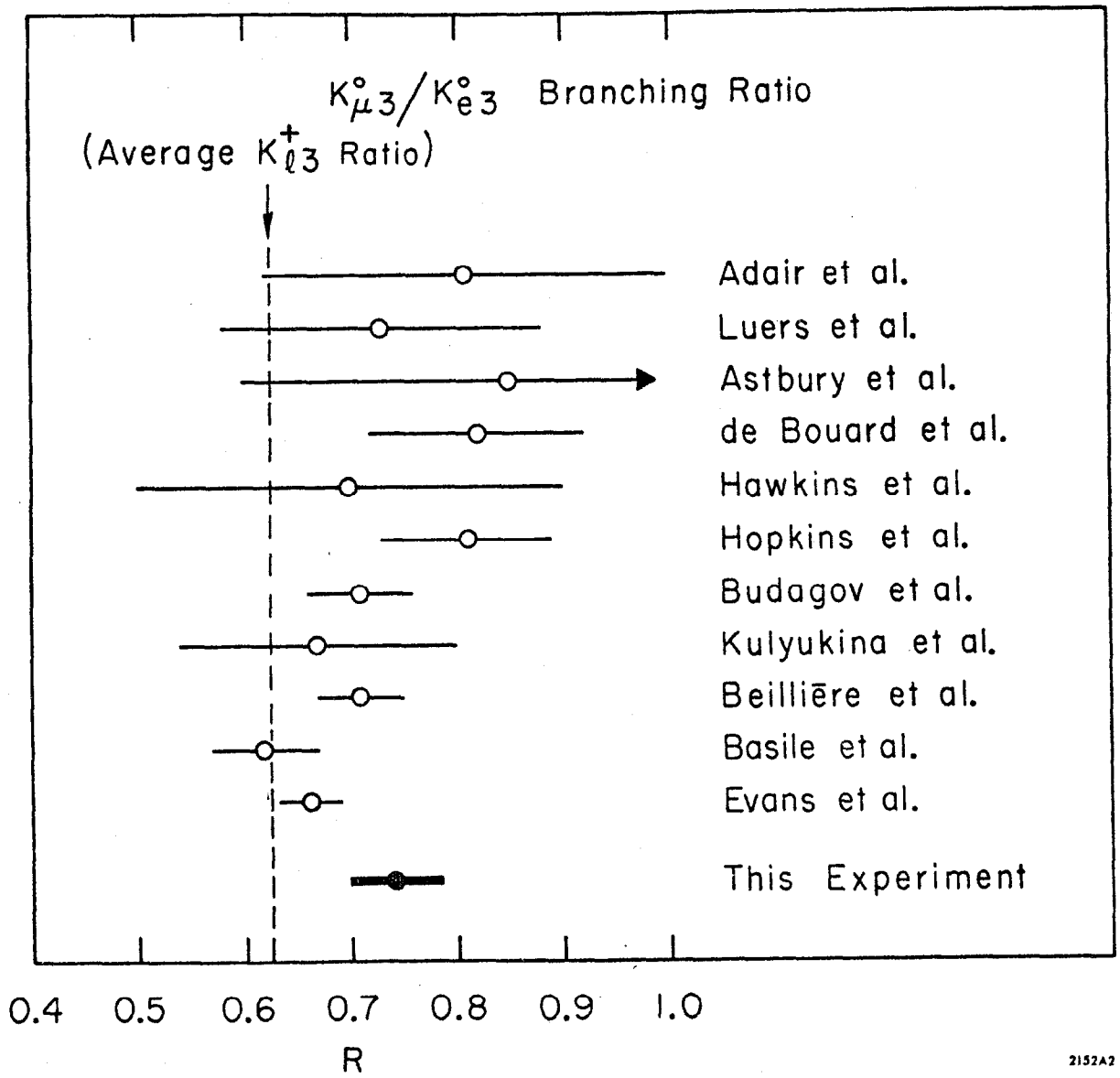
$K^0_{\mu 3}/K^0_{e3}$ Branching Ratio
(Average $K^+_{\ell 3}$ Ratio)
Adair et al.
Luers et al.
Astbury et al.
de Bouard et al.
Hawkins et al.
Hopkins et al.
Budagov et al.
Kulyukina et al.
Beilliēre et al.
Basile et al.
Evans et al.
This Experiment
0.4
0.5
0.6
0.7
0.8
0.9
1.0
R
2152A2

Fig. 12

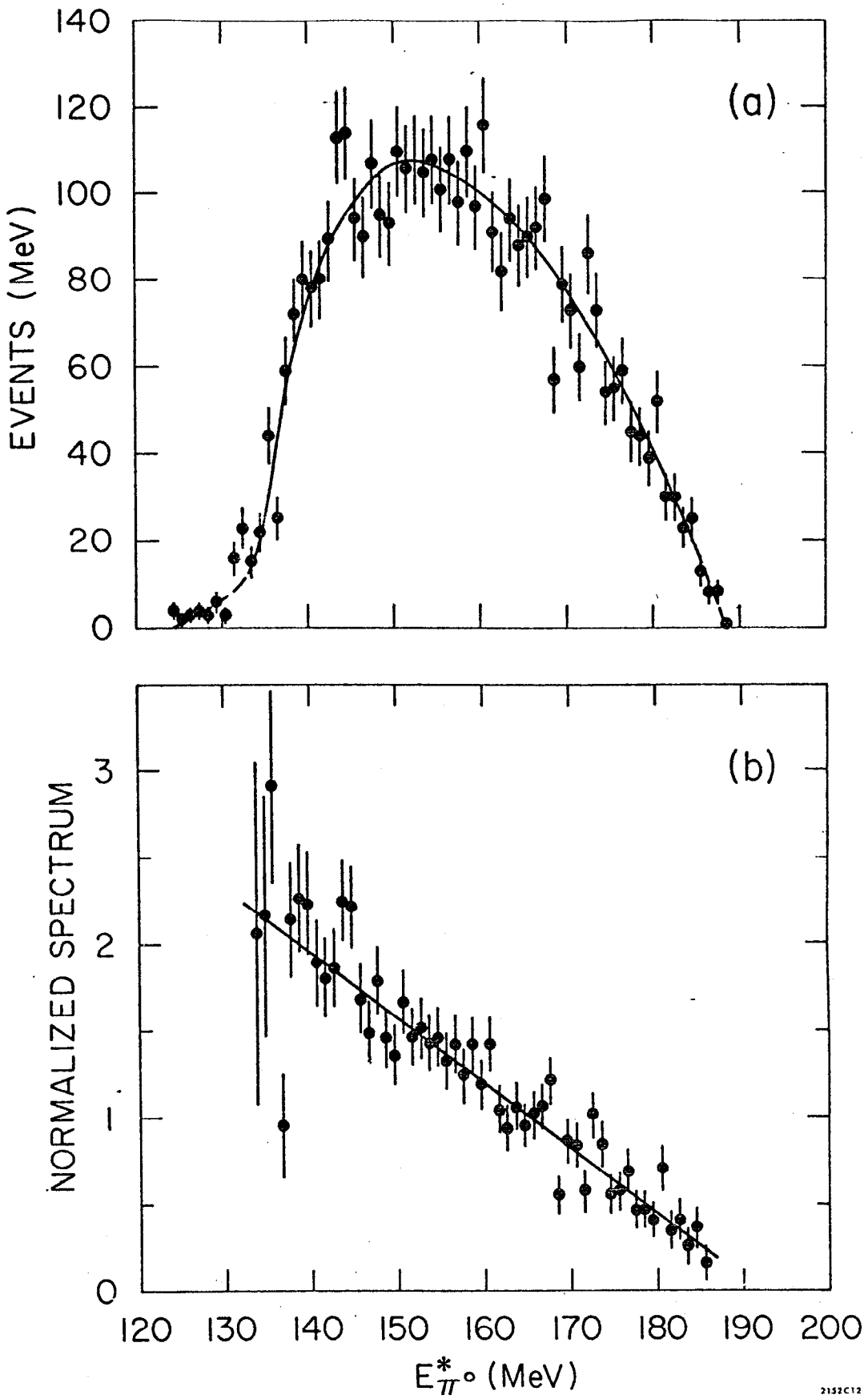
(a)
EVENTS (MeV)
140
120
100
80
60
40
20
0
(b)
NORMALIZED SPECTRUM
3
2
1
0
120
130
140
150
160
170
180
190
200
$E^*_{\pi^0}$ (MeV)
2132C12

Fig. 13